Supporting Information

Shimbo et al. 10.1073/pnas.1208616109

SI Text

Scripts 1-4 are available upon request.

Script 1. Converts html formatted results from Protein Prospector into a text file.

Script 2. Generates SRM transitions (parent ion and fragment ion pairs) for 5500QTRAP using output text files from Script 1. The top seven most intense fragment ions, *m/z* between 300 and 1,200, excluding Immonium ions, a_1, b_1, y_1, and fragments with *m/z* 2 Da of the precursor ion, were selected from the MS/MS spectrum for each identified peptide and the tentative collision energies were calculated as follows: for doubly charged precursor ions, [collision energy or CE (V)] = 0.03 × [*m/z* value] + 20; for triply charged precursor ions, [CE (V)] = 0.03 × [*m/z* value] + 18; for quadrivalant or more charged precursor ions, [CE (V)] = 0.013 × [*m/z* value] + 27. For each transition, a collision energy scan ([CE (V)] − 10, − 5, ± 0, + 5 and + 10) was performed to optimize CE values.

Script 3. Performs moving average smoothing with weighted Gaussian distribution for the five nearest data points. This script also adjusts the retention time.

Script 4. Calculates area-under-curve of each peptide peak.

SI Methods

Data Analysis and Bioinformatics. All of the data from scheduled SRM experiments were processed using in-house perl scripts (*SI Text*) and Microsoft Excel. The peptides were qualified by at least five of seven coeluting transitions on HPLC in one or more samples. For the peak intensity integration, three common observed transitions for each peptide were selected to calculate the area-under-the-curve (AUC). For quantitative analysis, the ratio of AUCs for the three common peaks were determined and if the rms was less than 0.4 and peak intensities less than $1.0e^4$, the peptide was discarded. The intensities from each sample were normalized with the average intensity of internal standards and total protein concentration (using a BCA assay). Cluster analyses were performed using Cluster (v3.0) and Java TreeView (v1.1.5r2). Go Miner was used for the GO analyses (1). To select specific peptides, averaged intensities were used to calculate *P* value from *t* test and fold-change against the other conditions. The scores were calculated from (Score) = $-\log_{10}(P) \times \log_2$(fold-change). Selected peptides listed in Table S2 and Table S3 scored greater 2 SDs from the averaged score.

Immunoblotting of Caspase Cleavages and Cell Viability Assays. Whole-cell lysates (1.0×10^7cells) were prepared in RIPA buffer (25 mMTris-HCl, 150 mM sodium chloride, 1% sodium deoxycholate, 0.1% SDS and 1% Triton X-100) containing the protease inhibitors (described above). The protein concentrations were measured by BCA method and 25 μg of protein were subjected to SDS/PAGE and transferred to nitrocellulose membranes. Blots were performed using the CREB-2 Antibody (sc-200; Santa Cruz Biotechnology) as the primary antibody and Amersham ECL-HRP Linked Secondary Antibodies (NA934; GE Healthcare).

1. Zeeberg BR, et al. (2003) GoMiner: A resource for biological interpretation of genomic and proteomic data. *Genome Biol* 4:R28.

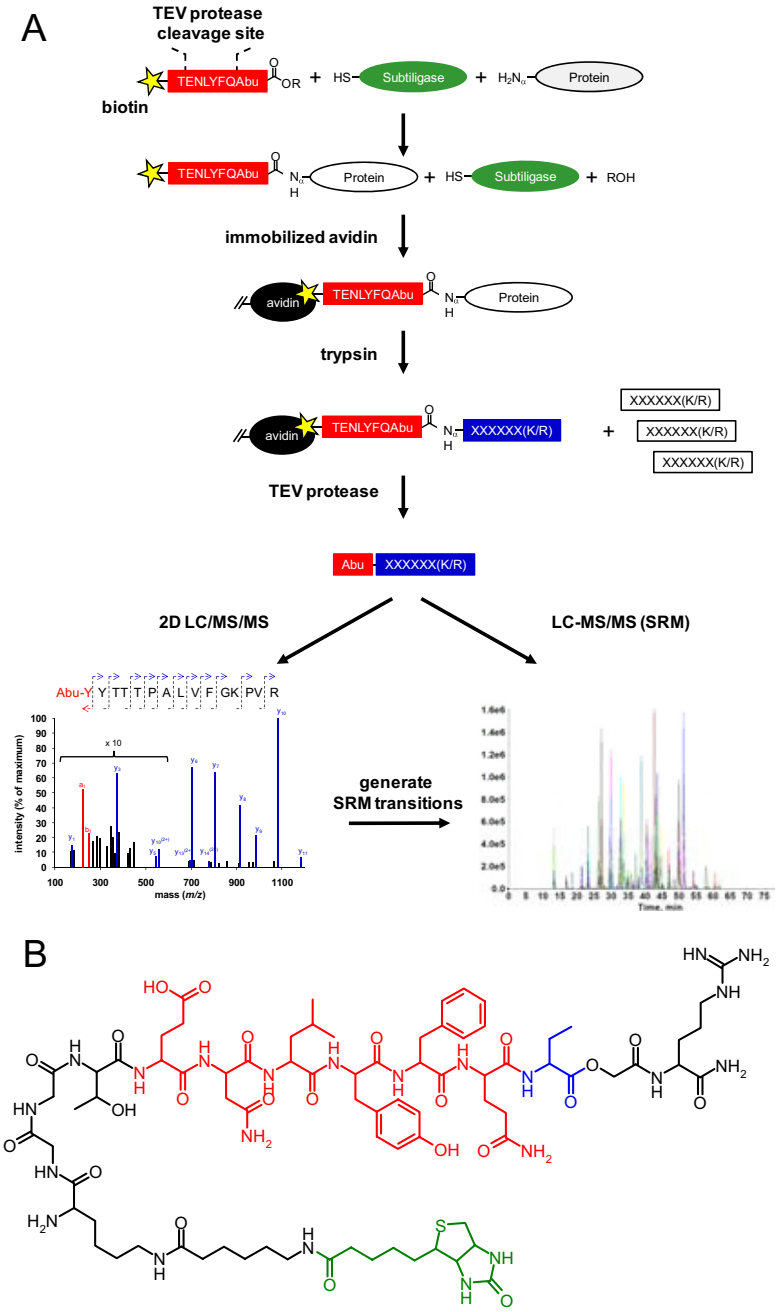

Fig. S1. Positive N-terminal enrichment strategy. (*A*) The free α-amines are labeled with biotinylated ester with the engineered enzyme subtiligase and captured on neutravidin beads. The peptides are cleaved by TEV (Tobacco etch virus) protease leaving an N-terminal remnant of the noncanonical amino acid, α-aminobutyric acid (Abu), which serves as a marker of subtiligase labeling. (*B*) TEVest4. The biotinylated ester, contains biotin (green), a α-aminohexanoic acid-di-glycine spacer, the TEV protease cleavage site (ENLYFQ, red), Abu (blue), and the ester, which is cleaved to generate the activated thiol-ester on subtiligase. Subtiligase then transfers Abu specifically to the α-amines on proteins and not ε-amines, free amino acids, or di-peptides (1).

1. Chang TK, Jackson DY, Burnier JP, Wells JA (1994) Subtiligase: A tool for semisynthesis of proteins. *Proc Natl Acad Sci USA* 91:12544–12548.

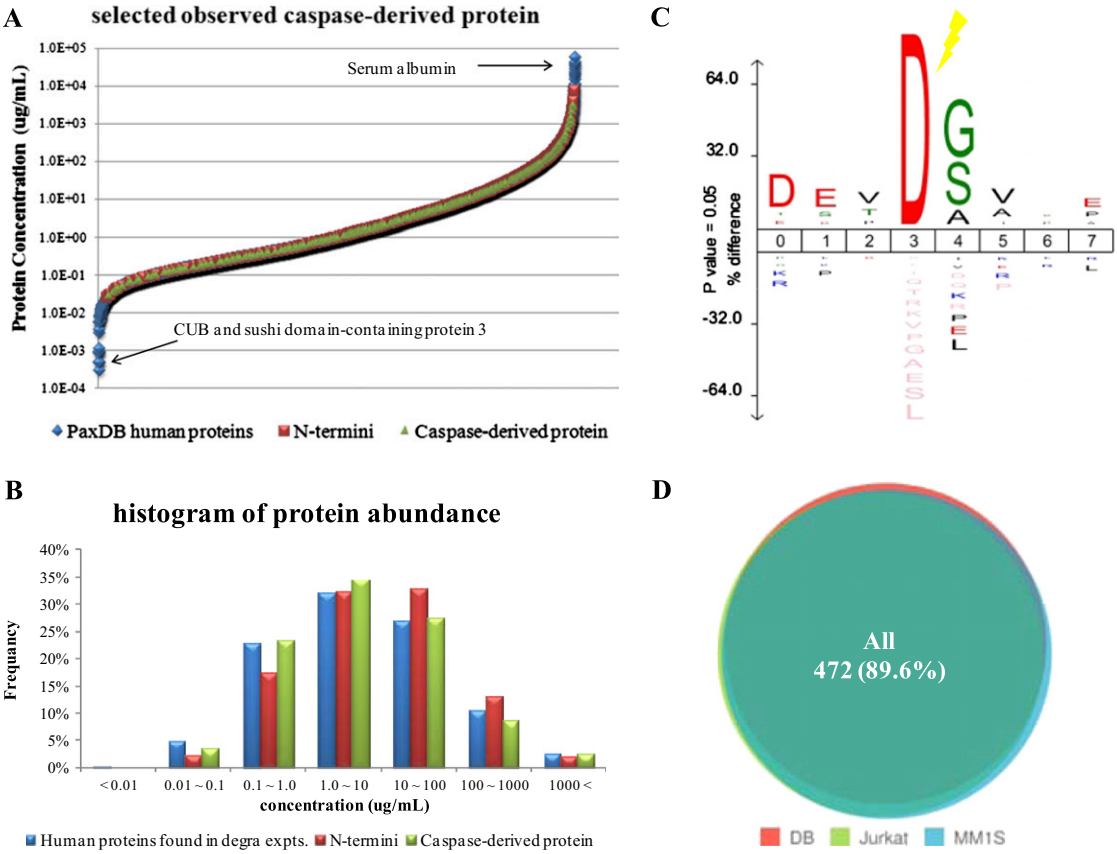

Fig. S2. Evaluation of stage 1 experiments. (*A*) Distribution of the identified proteins. Total observed N termini (red) and caspase-derived N termini (green) are plotted on the protein abundance data (blue) from PaxDb (pax-db.prg). Note that most of the high-abundance proteins are serum-derived and thus not expected to be present in our datasets. (*B*) Histogram of detected proteins versus their abundance. (*C*) IceLogo of the caspase-derived peptides from stage 1A. The amino acid frequency of the whole proteome annotated from the UniProt knowledge base was used to establish background frequency. IceLogo of caspase-derived peptides (aspartic acid at P1 position) showed the characteristic caspase cleavage site where cleavage occurs between aspartic acid and a small amino acid (1). The most common sequence from P4–P1 was DEVD, which is typical of caspases 3 and 7 (2). (*D*) Strong overlap of peptides (89.6%) detected in the three cell lines. Selected reaction monitoring (SRM) analysis of apoptotic cell lysates detected 488, 505, and 520 peptides in DB, Jurkat, and MM1S cell lines, respectively, with 472 peptides present in all three cell lines.

1. Colaert N, Helsens K, Martens L, Vandekerckhove J, Gevaert K (2009) Improved visualization of protein consensus sequences by iceLogo. *Nat Methods* 6:786–787.
2. Schechter I, Berger A (1968) On the active site of proteases. 3. Mapping the active site of papain; Specific peptide inhibitors of papain. *Biochem Biophys Res Commun* 32:898–902.

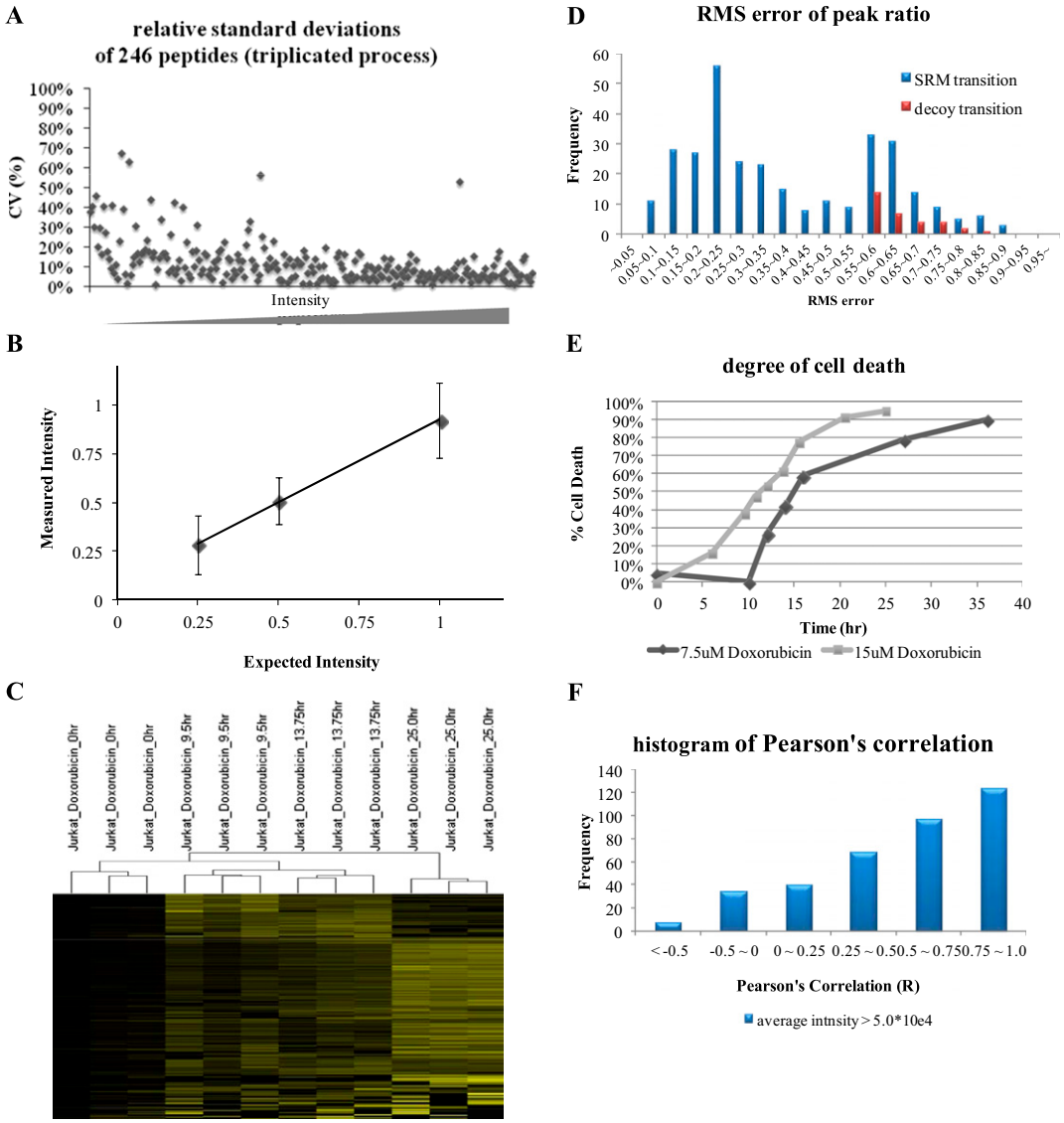

Fig. S3. Method validation for quantitative analysis. (*A*) Reproducibility of processing three individual ligations using same lysate. Averaged coefficient of variation (CV) was 12.3% for peptides with intensities >1.0 × 10e^4. (*B*) Linearity. Cell lysate were serially diluted, processed with subtiligase, and subjected to MS. The strong correlation suggests good reproducibility and linearity of response. (*C*) Analytical replication for three identical Jurkat cell samples treated with doxorubicin over four time points and processed for SRM analysis. An unbiased clustering algorithm groups the three replicates for each of the four time points. (*D*) Estimation of the false-discovery rates on SRM analysis. Decoy transitions were generated by randomizing amino acid sequence and comparing the relative signal intensity of the identified peptide transitions. No decoy transition had calculated rms errors > 0.5. All peptides classified as being quantified by SRM had calculated rms errors < 0.4. (*E* and *F*) Biological reproducibility. Jurkat cells were treated with two different doxorubicin concentrations and harvested at similar degrees of cell death (*E*) and a histogram of the Pearson's correlation coefficients for peptides with intensities > 5.0e10^4 is shown (*F*).

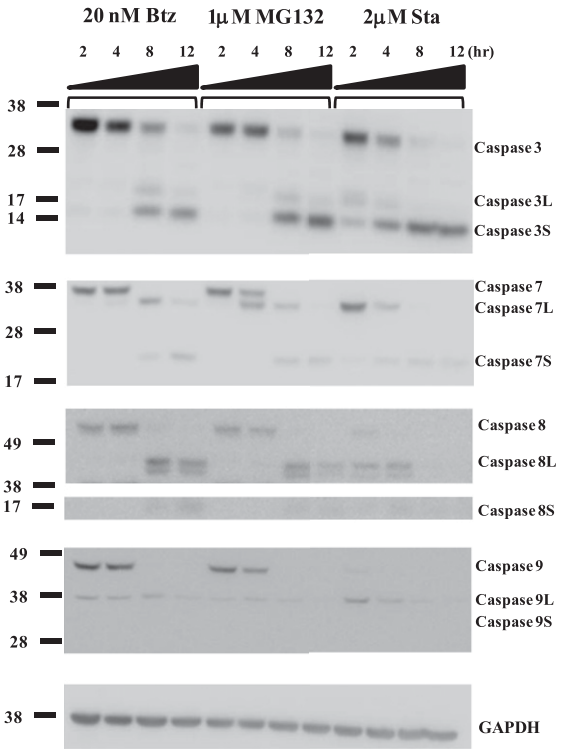

Fig. S4. Caspase activity profiles of MM1S. MM1S cells were treated with three different drugs: 20 nM bortezomib (Btz), 1 μM MG132, and 2μM staurosporine (Sta). Cells were harvested 2, 4, 8, and 12 h after the drug treatment. Immunoblots performed with antibodies to caspases 3, 7, 8, 9, and GAPDH are shown.

Table S1. Summary of caspase-derived peptides detected by SRM in stage 1B (three cell lines with two inducers) from 637 candidate sites discovered in stage 1A

Cell type	Drug			Total peptides (unique)
	Doxorubicin	Staurosporine	Bortezomib	
DB	444	472	—	488 (2)
Jurkat	499	478	—	505 (2)
MM1S	—	510	510	520 (6)

—, no data.

Table S2. Selected specific peptides and caspase targets unique to MM1S and Bortezomib in all three cell lines

Entry*	Protein names
MM1S cells	
Q15306_181	IFN regulatory factor 4
P47712_523	Cytosolic phospholipase A2
P04233_23	HLA class II histocompatibility antigen γ-chain
Q9H2L5_123	Ras association domain-containing protein 4
O60907_137	F-box-like/WD repeat-containing protein TBL1X
Q96MG2_13	Junctional sarcoplasmic reticulum protein 1
O43182_366	Rho GTPase-activating protein 6
P57764_276	Gasdermin-D
Q14157_851	Ubiquitin-associated protein 2-like
Bortezomib	
Q9H6S0_1084	Probable ATP-dependent RNA helicase YTHDC2
Q1KMD3_127	Heterogeneous nuclear ribonucleoprotein U-like protein 2
Q13541_26	Eukaryotic translation initiation factor 4E-binding protein 1
Q96GA3_206	Protein LTV1 homolog
Q9UMZ2_988	Synergin-γ
P63241_12	Eukaryotic translation initiation factor 5A-1
P18848_66	cAMP-dependent transcription factor ATF-4
Q9UBQ7_29	Glyoxylate reductase/hydroxypyruvate reductase
P51991_116	Heterogeneous nuclear ribonucleoprotein A3
O14787_354	Transportin-2
Q9NTJ3_25	Structural maintenance of chromosomes protein 4
Q7KZF4_189	Staphylococcal nuclease domain-containing protein 1
Q6ZUJ8_149	Phosphoinositide 3-kinase adapter protein 1
P23246_458	Splicing factor, proline- and glutamine-rich
P49792_3132	E3 SUMO-protein ligase RanBP2
P35749_1161	Myosin-11
Q9ULR0_168	Pre-mRNA-splicing factor ISY1 homolog
Q5T4S7_581	E3 ubiquitin-protein ligase UBR4
Q15181_166	Inorganic pyrophosphatase
Q12982_84	BCL2/adenovirus E1B 19 kDa protein-interacting protein 2
P35580_1161	Myosin-10

See *Methods* for scoring.
*UniProt accession number with position.

Table S3. Selected specific peptides

Entry*	Protein names
DB cells	
P14866_285	Heterogeneous nuclear ribonucleoprotein L
Q13451_186	Peptidyl-prolyl *cis-trans* isomerase FKBP5
P27797_122	Calreticulin
P04637_187	Cellular tumor antigen p53
Q9ULZ2_171	Signal-transducing adaptor protein 1
Q8IUI8_332	Cytokine receptor-like factor 3
Q04864_87	Proto-oncogene c-Rel
P21359_669	Neurofibromin
P84022_259	Mothers against decapentaplegic homolog 3
P55884_185	Eukaryotic translation initiation factor 3 subunit B
Q04206_98	Transcription factor p65
P20810_234	Calpastatin
P52565_144	Rho GDP-dissociation inhibitor 1
P27708_1887	CAD protein
Q8N999_60	Uncharacterized protein C12orf29
P49006_64	MARCKS-related protein
Q99615_9	DnaJ homolog subfamily C member 7
Jurkat cells	
P78559_1885	Microtubule-associated protein 1A
Q53F19_232	Uncharacterized protein C17orf85
P07602_313	Proactivator polypeptide
Q9Y6K1_439	DNA (cytosine-5)-methyltransferase 3A
Q92664_19	Transcription factor IIIA
P57764_88	Gasdermin-D
P21333_1337	Filamin-A
O43719_34	HIV Tat-specific factor 1
P23381_84	Tryptophanyl-tRNA synthetase, cytoplasmic
Q8WUA2_233	Peptidyl-prolyl *cis-trans* isomerase-like 4
Q9H8V3_629	Protein ECT2
Q86XP1_699	Diacylglycerol kinase η
Q96JM3_586	Zinc finger protein 828
Q92619_663	Minor histocompatibility protein HA-1
Q92917_38	G patch domain and KOW motifs-containing protein
O14686_387	Histone-lysine *N*-methyltransferase MLL2
Q96IZ7_239	Serine/Arginine-related protein 53
Q12888_830	Tumor suppressor p53-binding protein 1
Treatment with the proteasome inhibitor, Bortezomib or MG132	
P28070_30	Proteasome subunit β type-4
Q6FIF0_107	AN1-type zinc finger protein 6
P18848_66	cAMP-dependent transcription factor ATF-4
P47712_523	Cytosolic phospholipase A2
Q5JRA6_710	Melanoma inhibitory activity protein 3
Q9UMZ2_988	Synergin-γ
Q9H8Y5_135	Ankyrin repeat and zinc finger domain-containing protein 1
Q9UN37_231	Vacuolar protein sorting-associated protein 4A
P61978_351	Heterogeneous nuclear ribonucleoprotein K
Q8TCG2_15	Phosphatidylinositol 4-kinase type 2-β
Q13541_26	Eukaryotic translation initiation factor 4E-binding protein 1
Q96MG2_13	Junctional sarcoplasmic reticulum protein 1
Q9NZJ5_774	Eukaryotic translation initiation factor 2-α kinase 3
Q1KMD3_127	Heterogeneous nuclear ribonucleoprotein U-like protein 2
P63241_12	Eukaryotic translation initiation factor 5A-1
Q9ULR0_168	Pre-mRNA-splicing factor ISY1 homolog
Q9BTC0_410	Death-inducer obliterator 1
Q7L014_923	Probable ATP-dependent RNA helicase DDX46
Q8TEQ0_183	Sorting nexin-29
Treatment with the broad kinase inhibitor, staurosporine	
Q5BJE1_518	Uncharacterized protein C18orf34
Q14C86_1103	GTPase-activating protein and VPS9 domain-containing protein 1
P26368_129	Splicing factor U2AF 65-kDa subunit
Q96PK2_3523	Microtubule-actin cross-linking factor 1, isoform 4
Q2NKX8_1036	DNA excision repair protein ERCC-6-like

Table S3. Cont.

Entry*	Protein names
Q15365_221	Poly(rC)-binding protein 1
Q9H0H5_274	Rac GTPase-activating protein 1
P09496_77	Clathrin light chain A
Q9H5J8_11	TATA box-binding protein-associated factor RNA polymerase I subunit D
Q96G28_142	Coiled-coil domain-containing protein 104
Q9C0C9_438	Ubiquitin-conjugating enzyme E2 O
Q06210_261	Glucosamine–fructose-6-phosphate aminotransferase
P68363_70	Tubulin α-1B chain
Q7Z6I6_908	Rho GTPase-activating protein 30
P43243_681	Matrin-3
Q92917_38	G patch domain and KOW motifs-containing protein
P06400_347	Retinoblastoma-associated protein
Q9Y5A9_368	YTH domain family protein 2
O60784_158	Target of Myb protein 1
Q6NZY4_344	Zinc finger CCHC domain-containing protein 8
Q16576_99	Histone-binding protein RBBP7
Q15424_263	Scaffold attachment factor B1
Q14693_166	Phosphatidate phosphatase LPIN1
Q13136_219	Liprin-α-1
Q8N5W9_62	Protein FAM101B
P17544_44	cAMP-dependent transcription factor ATF-7
Treatment with the DNA damaging agent, doxorubicin	
P35637_356	RNA-binding protein FUS
P54252_218	Ataxin-3
P31939_340	Bifunctional purine biosynthesis protein PURH
P78559_1885	Microtubule-associated protein 1A
Q5T4S7_2904	E3 ubiquitin-protein ligase UBR4
P43686_298	26S protease regulatory subunit 6B
Q3B7T1_116	Erythroid differentiation-related factor 1
Q06546_16	GA-binding protein α-chain
Q8WYQ5_397	Microprocessor complex subunit DGCR8
Q13043_350	Serine/threonine-protein kinase 4
O15042_713	U2 snRNP-associated SURP motif-containing protein
P60709_158	Actin, cytoplasmic 1
Q8IW35_434	Centrosomal protein of 97 kDa
P25205_702	DNA replication licensing factor MCM3
O75533_35	Splicing factor 3B subunit 1
Q9Y2X3_125	Nucleolar protein 58
O43719_34	HIV Tat-specific factor 1
Q96SB3_552	Neurabin-2
Q96B23_45	Uncharacterized protein C18orf25
O94913_1289	Pre-mRNA cleavage complex 2 protein Pcf11
P21333_1049	Filamin-A
Q92619_40	Minor histocompatibility protein HA-1
P17980_28	26S protease regulatory subunit 6A
Q5JSZ5_1777	Protein PRRC2B
Q12888_318	Tumor suppressor p53-binding protein 1
P35251_724	Replication factor C subunit 1
O14974_73	Protein phosphatase 1 regulatory subunit 12A

Caspase targets specific for DB and Jurkat cells, and treatment with proteasome inhibitors Bortezomib or MG132, staurosporine, or doxorubicin. See *Methods* for scoring.
*UniProt accession number with position.

Table S4. Proteins correlated to degree of cell death among all conditions (average $R > 0.75$ and minimum $R > 0.5$)

Entry*	Protein names	Averaged *R*	Catalytic efficiency†
O43719_40	HIV Tat-specific factor 1	0.87	✓
O60664_220	Perilipin-3	0.86	✓
Q14839_1234	Chromodomain-helicase-DNA-binding protein 4	0.85	
Q92945_129	Far upstream element-binding protein 2	0.84	✓
Q96MG7_42	Melanoma-associated antigen G1	0.83	✓
Q13614_49	Myotubularin-related protein 2	0.83	
Q07666_76	KH domain-containing, RNA-binding, signal transduction-associated protein 1	0.83	✓
P61978_129	Heterogeneous nuclear ribonucleoprotein K	0.82	✓
Q14498_332	RNA-binding protein 39	0.81	✓
Q92538_369	Golgi-specific brefeldin A-resistance guanine nucleotide exchange factor 1	0.80	
Q8N1F7_158	Nuclear pore complex protein Nup93	0.78	✓
Q15154_194	Pericentriolar material 1 protein	0.77	
Q8N3X1_154	Formin-binding protein 4	0.77	
P45974_783	Ubiquitin carboxyl-terminal hydrolase 5	0.77	✓
Q9GZR7_297	ATP-dependent RNA helicase DDX24	0.76	

*UniProt accession number with position
†Described as higher catalytic efficiencies for caspases (ref. 1)

1. Agard NJ, et al. (2012) Global kinetic analysis of proteolysis via quantitative targeted proteomics. *Proc Natl Acad Sci* 109:1913–1918.

Dataset S1. List of N-terminal peptides identified from apoptotic cells in stage 1A discovery experiment

Dataset S1

Dataset S2. Generated SRM transitions for QTRAP 5500

Dataset S2

Control peptides are in bold.

Dataset S3. Calculated intensities of SRM results from stages 1 and 2

Dataset S3

(*A*) Calculated intensities of SRM results from stage 1B. (*B*) Calculated intensities of SRM results from stage 2 (in bold are the 628 peptides shown in Fig. 2).